JACS Au
AN OPEN ACCESS JOURNAL OF THE AMERICAN CHEMICAL SOCIETY

pubs.acs.org/jacsau

Article

DFT Study on the Biosynthesis of Verrucosane Diterpenoids and Mangicol Sesterterpenoids: Involvement of Secondary-Carbocation-Free Reaction Cascades

Hajime Sato,* Bi-Xiao Li, Taisei Takagi, Chao Wang, Kazunori Miyamoto, and Masanobu Uchiyama*

Cite This: *JACS Au* 2021, 1, 1231−1239

Read Online

ACCESS | Metrics & More | Article Recommendations | Supporting Information

ABSTRACT: Some experimental observations indicate that a sequential formation of secondary (2°) carbocations might be involved in some biosynthetic pathways, including those of verrucosane-type diterpenoids and mangicol-type sesterterpenoids, but it remains controversial whether or not such 2° cations are viable intermediates. Here, we performed comprehensive density functional theory calculations of these biosynthetic pathways. The results do not support previously proposed pathways/mechanisms: in particular, we find that none of the putative 2° carbocation intermediates is involved in either of the biosynthetic pathways. In verrucosane biosynthesis, the proposed 2° carbocations (**II** and **IV**) in the early stage are bypassed by the formation of the adjacent 3° carbocations and by unusual skeletal rearrangement reactions, and in the later stage, the putative 2° carbocation intermediates (**VI**, **VII**, and **VIII**) are not present as the proposed forms but as nonclassical structures between homoallyl and cyclopropylcarbinyl cations. In the mangicol biosynthesis, one of the two proposed 2° carbocations (**X**) is bypassed by a C−C bond-breaking reaction to generate a 3° carbocation with a C=C bond, while the other (**XI**) is bypassed by a strong hyperconjugative interaction leading to a nonclassical carbocation. We propose new biosynthetic pathways/mechanisms for the verrucosane-type diterpenoids and mangicol-type sesterterpenoids. These pathways are in good agreement with the findings of previous biosynthetic studies, including isotope-labeling experiments and byproducts analysis, and moreover can account for the biosynthesis of related terpenes.

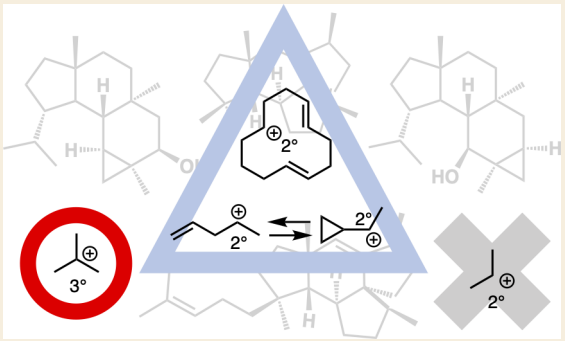

KEYWORDS: *terpene, biosynthesis, carbocation cascade, DFT study, nonclassical structure*

INTRODUCTION

Terpenes/terpenoids are fascinating compounds due to their complicated and diverse structures and wide range of bioactivities. They are biosynthesized from simple unsaturated hydrocarbons via successive carbocation-mediated reactions triggered by terpene cyclases.[1] A detailed knowledge of their biosynthetic mechanisms would be very helpful for understanding the evolution of particular biosynthetic pathways as well as for designing new biosynthetic routes for complex functional molecules. However, the mechanistic issues are extremely difficult to resolve fully by means of experimental studies alone, since terpene cyclization is a domino-type reaction occurring inside a single enzyme ("black box"). We recently established a powerful combination of quantum-chemical calculations with the artificial force induced reaction (AFIR) method[2,3] to unveil complicated biosynthetic pathways/mechanisms, such as those leading to trichobrasilenol,[4] quiannulatene,[5] and cyclooctatin.[6,7] In general, experimental and theoretical studies indicate that a terpene biosynthesis involves a sophisticated exothermic cascade of reactions, in which carbocation intermediates are converted into more stable intermediates such as allyl cations, tertiary (3°) carbocations, and cycloalkylcarbinyl cations. On the basis of experimental observations, it has been proposed that secondary (2°) carbocation intermediates play a role in some cases, such as in the biosynthesis of verrucosane-type diterpenoids and mangicol-type sesterterpenoids, but it remains controversial whether such 2° cations are viable intermediates. The stability of carbocations is one of the most important concepts in organic chemistry, and their stability relationships are fundamental to understanding many aspects of the reactivity of organic molecules/intermediates. For example, experimental studies show that *sec*-Bu^+ is 14.5 kcal mol^{-1} more unstable than *tert*-Bu^+.[8−11] Therefore, it is of considerable interest to verify the putative involvement of 2° carbocations in the biosynthesis of natural products.

Received: April 23, 2021
Published: July 9, 2021

https://doi.org/10.1021/jacsau.1c00178
JACS Au 2021, 1, 1231−1239

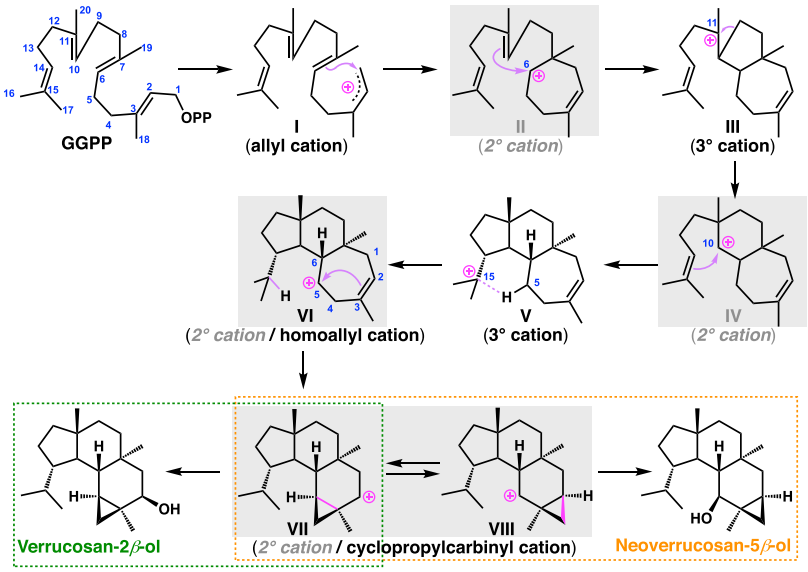

Figure 1. Proposed biosynthetic pathways of verrucosan-2β-ol and neoverrucosan-5β-ol.

Verrucosane-type Diterpenoids

Verrucosan-2β-ol (**ver**) and neoverrucosan-5β-ol (**neo**), featuring a unique 3,6,6,5-tetracyclic system, are diterpenoids isolated from *Chloroflexus aurantiacus*, a filamentous, gliding, thermophilic phototrophic bacterium.[12] Rieder et al. extensively investigated the biosynthetic pathway of verrucosan-2β-ol by means of an *in vivo* incorporation of singly or doubly ^{13}C-labeled acetate, and they proposed a biosynthetic pathway involving the formation of many secondary carbocations (**II**, **IV**, **VI**, **VII**, and **VIII**) (Figure 1).[13,14] Another important issue is to identify the bifurcation mechanism leading to the **ver** and **neo** skeletons.[15] At the bifurcation point, a unique C−C bond rearrangement via a cyclopropylcarbinyl cation was proposed. A similar skeletal rearrangement is seen in the cyclooctatin biosynthesis.[6,7] However, the key cyclopropylcarbinyl/homoallyl cation intermediates in cyclooctatin biosynthesis are categorized as 3° carbocations, whereas those in the proposed verrucosane-type biosynthesis are all 2° cations (**VI**, **VII**, and **VIII**).

Mangicol-type Sesterterpenoids

Mangicols are a family of marine fungal sesterterpenoids with a unique 6,5,5-spirotricyclic skeleton (Figure 2A),[16,17] isolated from *Fusarium heterosporum*, and they show weak cytotoxicity toward various cancer cell lines. On the basis of experimental studies, the biosynthetic pathway shown in Figure 2B was proposed,[16,17] involving the successive formation of two 2° carbocations (**X** and **XI**).

We began our study by evaluating the proposed pathways of verrucosane and mangicol biosynthesis with density functional theory (DFT) calculations. Since the results did not support the involvement of the proposed 2° carbocations, we then comprehensively explored the biosynthetic pathways by means of DFT calculations combined with the AFIR method. On the basis of these findings, we propose new routes that are in good agreement with previous experimental biosynthetic studies and also provide plausible pathways for the formation of other related terpenes/terpenenoids.

COMPUTATIONAL METHODS

All calculations were performed with GRRM11[2,18−21] based on the Gaussian 16 program.[22] Structure optimizations were performed at the M06-2X level in the gas phase using the 6-31+G(d,p) basis set.[23] The vibrational frequencies were computed at the same level to check whether each optimized structure is an energy minimum (no imaginary frequency) or a transition state (single imaginary frequency). Intrinsic reaction coordinates (IRC) calculations[24−27] were performed to track minimum energy paths from transition structures to the corresponding local minima. Single-point energies were calculated at the mPW1PW91/6-31+G(d,p) level[28,29] based on the structures optimized by the M06-2X method. The Gibbs free energy used for discussion in this study was calculated by adding the gas-phase Gibbs free energy correction.

RESULTS AND DISCUSSION

Verrucosane-type Biosynthesis

We first discuss the biosynthetic pathway of verrucosane-type diterpenoids. A systematic search of reaction pathways showed that the reaction **IM0** → **IM7** depicted in Figure 3A is the most favorable pathway. The dissociation of pyrophosphate followed by an *E*/*Z* isomerization[30,31] initiates the exothermic carbocation cascade of verrucosane biosynthesis and yields an allylic carbocation (**IM0**). Then, the C3−C4 single bond rotates with a small activation barrier of 4.9 kcal mol^{-1} so that the C1 carbon can interact directly with the C6−C7 π bond to afford the 3° carbocation intermediate (**IM1**). As can be seen from the elongated C1−C6 bond distance (1.63 Å) as well as the natural population analysis (NPA) charges on C3 (+0.04) and C11 (+0.04), the 3° carbocation (+0.48) at the C7 position is partially stabilized by the C1−C6 σ bond and the distal C2−C3/C10−C11 π bonds. Thus, the monocyclic six-membered 3° cation **IM1** undergoes a smooth skeletal rearrangement to afford 7,5-bicyclic 3° cation (**IM2**) in a single step with a large stabilization energy. A close examination of the IRC calculation results revealed that this step is actually concerted but involves two asynchronous events, namely, (1) a reverse (3° → 2° cation) Wagner-Meerwein rearrangement (ring expansion to give the 7-membered ring) and (2) an annulation to yield the 7,5-bicyclic system. Notably, the experimentally supported

https://doi.org/10.1021/jacsau.1c00178
JACS Au 2021, 1, 1231−1239

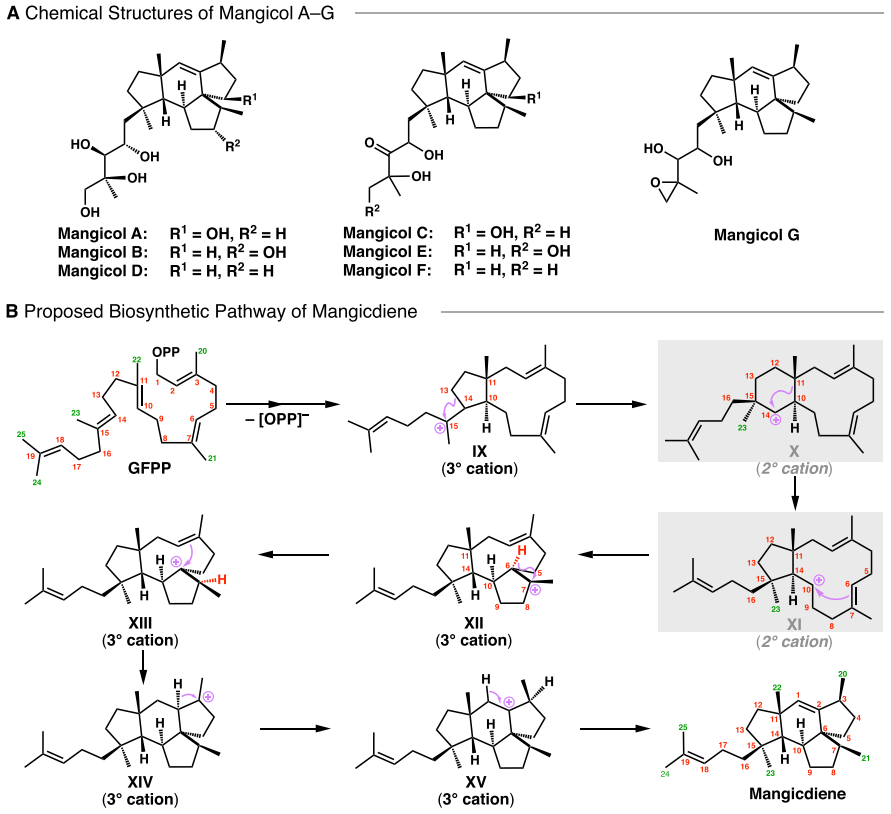

Figure 2. (A) Chemical structures of mangicol A–G. (B) Proposed mechanism of mangicdiene biosynthesis.

monocyclic seven-membered secondary carbocation structure (Figure 1, **II**) is not a minimum on the potential energy surface (PES). A conformational change of **IM2** with an activation barrier of only 1.0 kcal mol^{-1} yields **IM3**, in which the 3° cation center is further stabilized by a cation-σ bond interaction assisted by the distal C14–C15 π bond, leading to the second skeletal rearrangement to afford 7,6,5-tricyclic 3° carbocation intermediate (**IM4**). Again, the experimentally supported 7,6-bicyclic 2° carbocation structure (Figure 1, **IV**) is not located. Thus, the proposed intermediary 2° carbocations in the early stage of the biosynthesis are bypassed by the formation of the adjacent 3° carbocations together with skeletal rearrangement via a kind of nonclassical carbocation interaction with a through-space participation of the C–C σ bond and the distal π bond. Note that, in these skeletal rearrangement processes (**IM1** → **IM2**/**IM3** → **IM4**), a direct attack of the corresponding (C10–C11/C14–C15) π electrons on the 3° carbocation centers (at C7/C11) does not occur due to the destabilization associated with a four-membered ring formation. From **IM4**, a 1,5-H shift takes place with a reasonable activation energy of 6.7 kcal mol^{-1} to migrate the isopropyl 3° cation to a homoallyl cation in a seven-membered ring (**IM5**) with a slight endothermicity. As judged from the NPA charge distributions and the bond lengths, we consider **IM5** to be an intermediate structure between the homoallyl cation and the corresponding cyclopropylcarbinyl cation. The cyclopropylcarbinyl cation has highly distorted cyclopropane C–C σ bonds that can effectively stabilize the adjacent carbocation. Indeed, it has been reported that homoallyl/cyclopropylcarbinyl 3° cations play pivotal roles as stable intermediates in various stages of brasilane-type sesquiterpene[3] and cyclooctatin-type diterpene biosynthesis.[6,7] It is noteworthy that these were all 3° cations, whereas **IM5** is a more unstable 2° cation, presumably reflecting the nonclassical intermediate (equilibrium) structure. Finally, an unusual C–C bond rearrangement takes place via a highly distorted bicyclobutonium 3° cation[32,33] (**IM6**) with very low activation energy to give another homoallyl-cyclopropylcarbinyl intermediate structure (**IM7**). **IM7** is slightly more stable than **IM5** by 3.7 kcal mol^{-1}, probably owing to hyperconjugation from neighboring moieties. The energy diagram (Figure 3B) immediately suggests that this is a thermodynamically and kinetically favorable biosynthetic reaction cascade: (1) the activation barriers are all low enough for the reactions to proceed smoothly at ambient temperature, (2) the entire energy profile descends as the reactions proceed, and (3) the overall exothermicity is very large (ca. 40 kcal mol^{-1}). Any of the three skeletal rearrangements (**IM1** → **TS_1–2**/**IM3** → **TS_3–4**/**IM5** → **TS_5–6**) could be the rate-determining step.

Mangicol-type Biosynthesis

Next, we discuss in detail the biosynthesis of mangicol-type sesterterpenoids. Only a few C20/C25 terpenoids based on 5,11-bicyclic systems, such as ophiobolin,[34,35] cotylenin A,[36] and fusicoccadiene,[37] have been reported,[38] in contrast to those derived from 5,15-systems, such as quiannulatene,[5,39] sesterfisherol,[40,41] (+)-astellatene,[42,43] arathanadiene derivatives, sestermobaraenes,[44] and aspergildienes.[45] In the present study, **IM8** was adopted as the simplest chemical model (Figure 4).[46−49] The reaction pathway for the conversion of **IM8** into **IM11** is shown in Figure 4A, together with the relative energies with respect to **IM8**. The generation of allyl cation **IM8**, upon the loss of pyrophosphate of **SM**, triggers the carbocation cyclization cascade and affords a 5,11-bicyclic intermediate **IM9a**, which is a 3° carbocation intermediate, as

https://doi.org/10.1021/jacsau.1c00178
JACS Au 2021, 1, 1231−1239

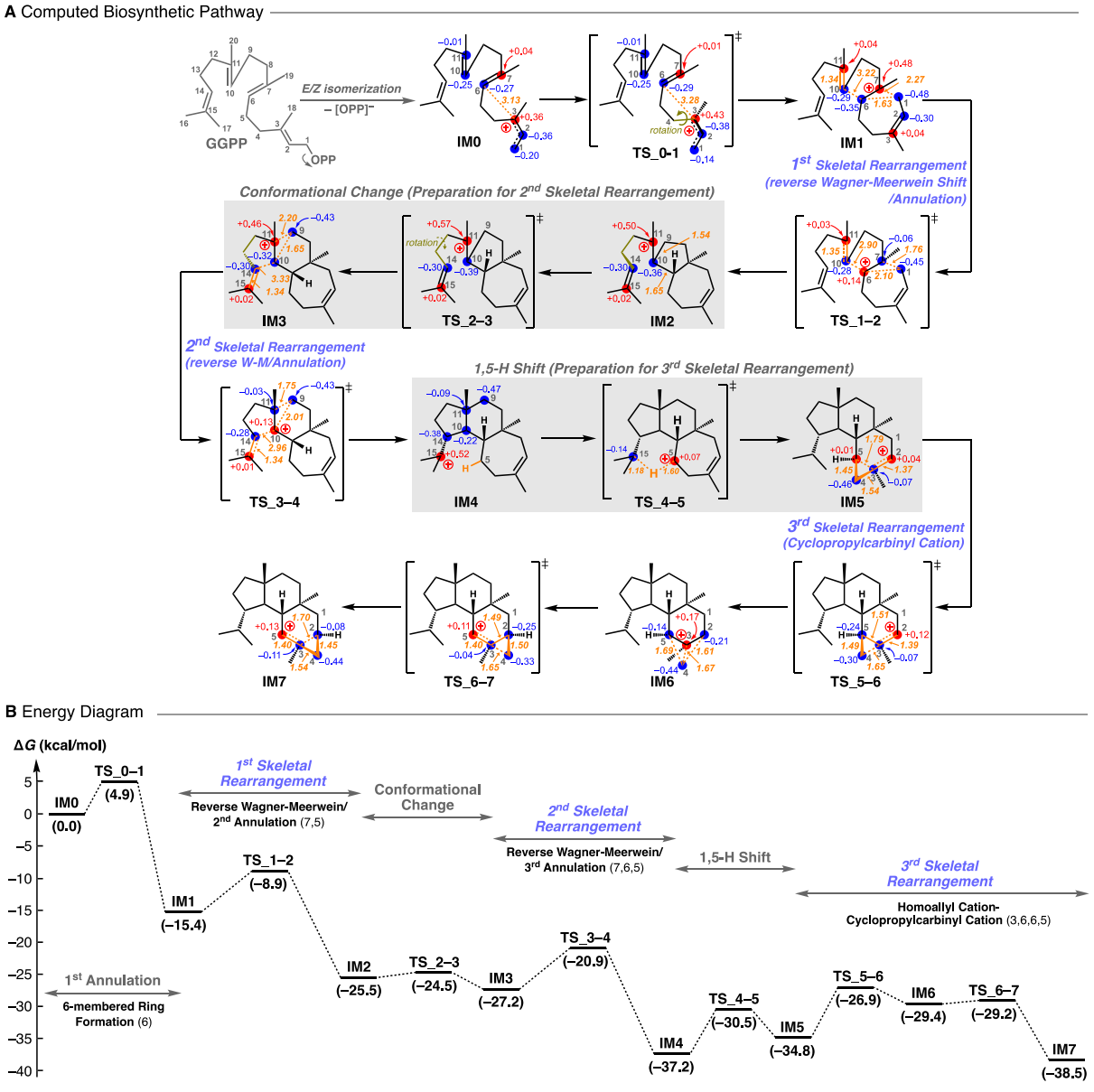

Figure 3. Results of a DFT evaluation of (A) the whole biosynthetic pathway and (B) the energy diagram of verrucosane. **IM** stands for intermediate. **TS** stands for transition state. Potential energies (kcal mol^{-1}, Gibbs free energies calculated at the mPW1PW91/6-31+G(d,p) level based on M06-2X/6-31+G(d,p) geometries) relative to **IM0** are shown in parentheses.

generally found in terpene biosynthesis. After the conformational change of **IM9a** to **IM9b** with an activation barrier of only 0.2 kcal mol^{-1}, an unusual C−C bond cleavage to afford the monocyclic 15-membered 3° carbocation **IM10a** proceeds in a single step from the 5/11 bicyclic structure via **TS_9b−10a** with an activation energy of 11.3 kcal mol^{-1}. Notably, the experimentally supported 6,11-bicyclic 2° carbocation structure (**X**) is not a minimum on the PES.[16,17] We anticipated that the present skeletal rearrangement would involve two asynchronous events, namely, (1) the 1,2-alkyl shift (ring expansion to give 6,11-bicyclic skeleton) and (2) the unusual C−C bond cleavage. Indeed, we found the corresponding peaks (**shoulder_9b−10a-1** and **shoulder_9b−10a-2**, respectively) located before and after the main peak (**TS_9b−10a**) upon a close examination of the IRC analysis results (Figure 4B). As judged from the elongated C10−C11 (1.65 Å) and C13−C15 (1.65 Å) bond distances as well as the near linearity of the C10−C14−C15 moiety (dihedral angles of empty orbital of C14 with C10−C11 and C13−C15: 165.8° and 176.5°, respectively), we consider that **shoulder_9b−10a-1** is close to the putative 2° carbocation structure in which the carbocation at C14 is partially stabilized by hyperconjugative interactions with the C10−C11 and C13−C15 σ bonds. If the C13−C15 bond were broken, a primary (1°) carbocation would be generated at C13, which would be very unstable.[50,51] Hence, the C10−C11 bond is elongated (while the C13−C15 bond is shortened) to provide **TS_9b−10a**, leading to the formation of a stable 3° carbocation at C11 (**IM10**). Note that the distance between the C10−C14 double bond and 3° cation center C11 in **IM10a** is more than 3 Å, and there are NPA charges at C10 (−0.18) and C14 (−0.25), suggesting little or no interaction between these locations. **IM10a** has a homoallylic 3° carbocation moiety. Thus, **IM10a** is converted via **TS_10a−10b** to a more stable cyclopropylcarbinyl 3° cation **IM10b**, of a type that is often observed in various stages of brasilane-type sesquiterpene,[4] cyclooctatin-type diterpene,[6,7]

https://doi.org/10.1021/jacsau.1c00178
JACS Au 2021, 1, 1231−1239

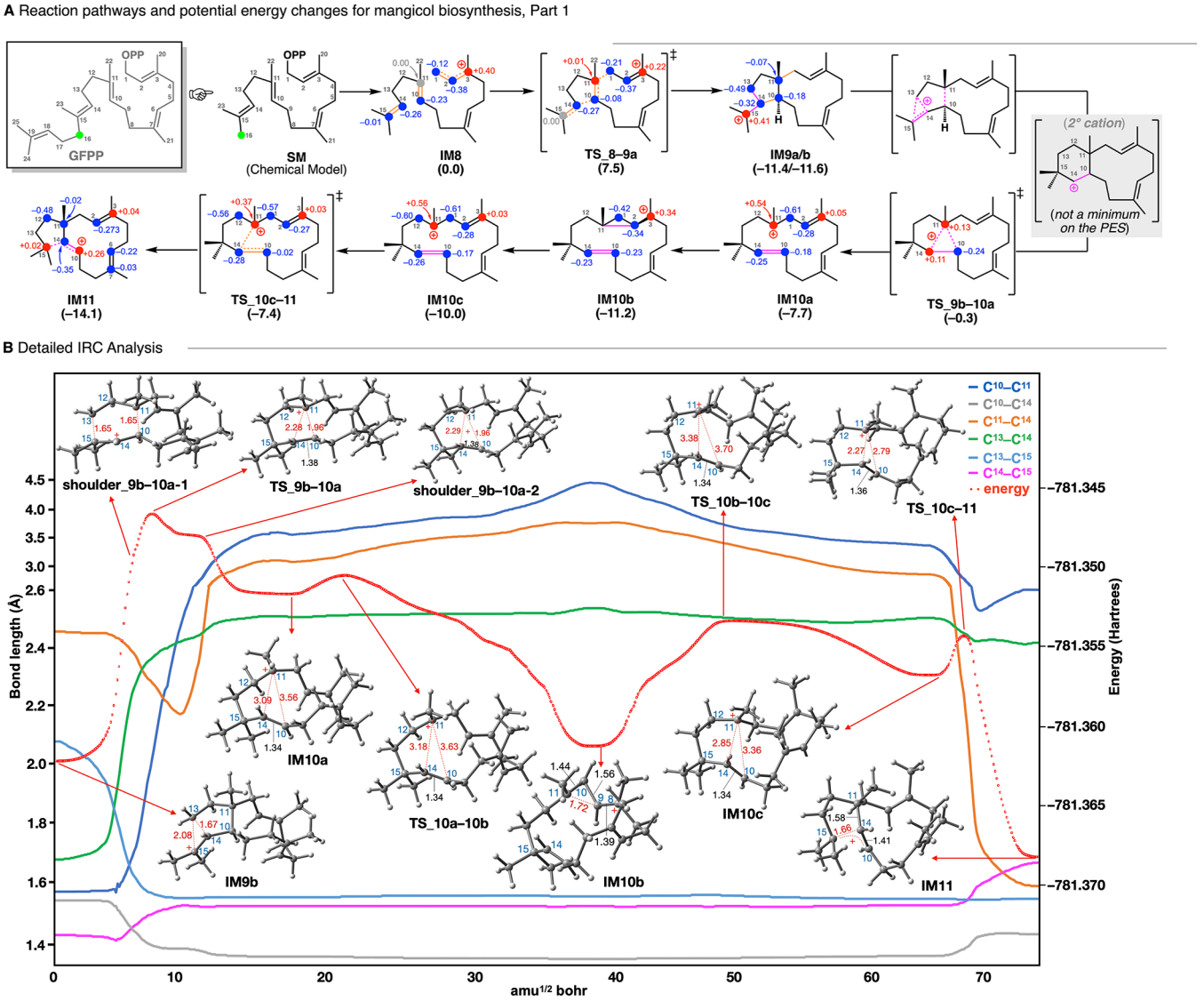

Figure 4. (A) Reaction pathways and potential energy changes from **IM8** to **IM11** (early stage of mangicol biosynthesis). The numberings are derived from those of GFPP. Potential energies (kcal mol^{-1}, Gibbs free energies calculated at the mPW1PW91/6-31+G(d,p) level based on M06-2X/6-31+G(d,p) geometries) relative to **IM8** are shown in parentheses. (B) A representative example of the evolution of key bond lengths in the conversion of **IM9b** to **IM11**.

and isoafricanol biosynthesis.[52] Thus, **IM10** has three equilibrium structures within ca. 4 kcal mol^{-1}, and interconversion (conformational change) between homoallyl carbocations **IM10a** and **IM10c** proceeds via viacyclopropylcarbinyl cation **IM10b**. Then, a cation-mediated transannular cyclization takes place from the reactive conformer **IM10c** to form the 5,12-bicyclic system **IM11** with a very low activation energy (2.6 kcal mol^{-1}). Intermediate **IM11** has an elongated C14−C15 single bond (1.66 Å) and C10−C14 double bond (1.41 Å), reflecting the partial breakdown of the C−C σ bond (1.54 Å) and π bond (1.34 Å), respectively. This suggests a nonclassical structure[8,53] between the monocyclic 3° cation and bicyclic humulyl 2° cations, leading to the following multiple annulations (*vide infra*). A similar reaction is also found in variediene biosynthesis.[54,55]

We next located the later stage of mangicol biosynthesis, that is, the formation of the spirotricyclic structure (Figure 5). Route A is very similar to the previously proposed pathway, in which the annulation of **IM11** takes place to give 5,9,5-tricyclic intermediate **IM12** having B- and D-rings with a slight endothermicity, followed by 1,2-H shift via **TS_12−13** with a large stabilization energy to give the bridgehead 3° carbocation **IM13**. From **IM13**, a smooth annulation involving conformational change of the nine-membered ring and 1,2-H shift proceeds to construct the 6,5,5-spirotricyclic skeleton **IM14a** in a single step with a large exothermicity. Then, **IM14a** is subjected to deprotonation to give the mangicol core skeleton (**PD**). The energy profile is consistent with the previously proposed pathway (Figure 2B), with reasonable activation barriers (all low enough for the reactions to proceed smoothly at ambient temperature) and with an overall large exothermicity (over 35 kcal mol^{-1}). However, another unprecedented route, Route B (via 5,6,5,5-tetracyclic intermediate **IM17** having A- and D-rings), which was located by application of the AFIR method for comprehensive searching of reaction paths, turned out to be the most favorable (Figure 5B). As supported by the NPA charge distribution of **IM11**, where C10 (+0.26) and C3 (+0.04) are more positive than the

https://doi.org/10.1021/jacsau.1c00178
JACS Au 2021, 1, 1231−1239

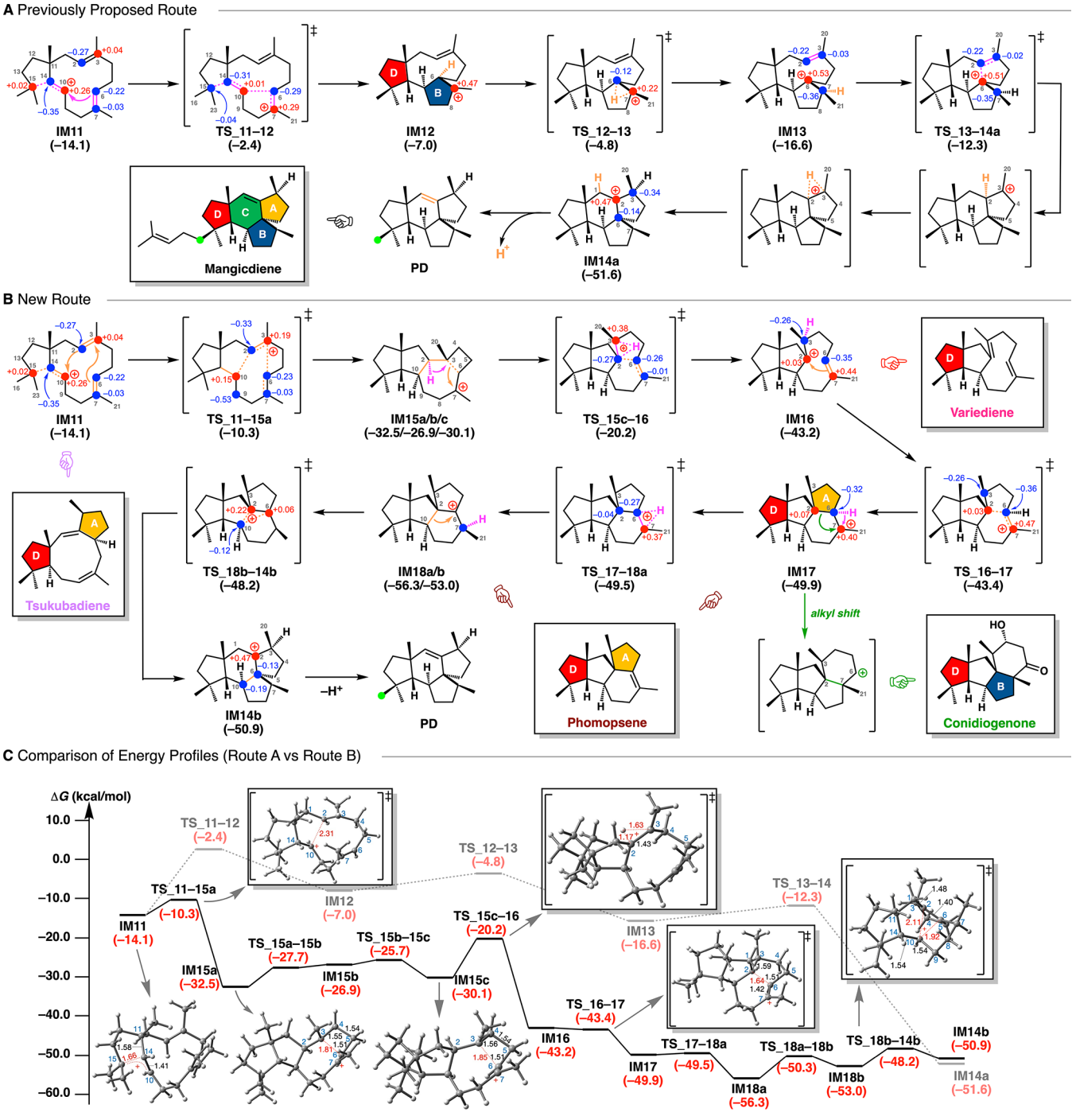

Figure 5. Reaction pathways and potential energy changes from **IM11** to **PD** (later stage of mangicol biosynthesis, Part 2). See Figure 3 for details. (A) Previously proposed route. (B) New route. (C) Comparison of the energy profiles of route A (dashed line) and route B (solid line). Potential energies (kcal mol^{-1}, Gibbs free energies calculated at the mPW1PW91/6-31+G(d,p) level based on M06-2X/6-31+G(d,p) geometries) relative to **IM8** are shown in parentheses.

C6 and C7 carbons, cation-stitching multiple annulation initiates this pathway with a very low activation energy (3.8 kcal mol^{-1}) to form the 5,5,7,4-tetracyclic intermediate **IM15a** with a large exothermicity (22.2 kcal mol^{-1}), in which the highly distorted cyclobutane C3−C6 bond effectively stabilizes the adjacent C7 carbocation.[56] Thus, after the interconversion from **IM15a** to **IM15c**, a 1,2-H shift takes place smoothly to give a 5,5,9-tricyclic 3° cation (**IM16**) stabilized by a cation-π interaction[3,57] with the newly generated C6−C7 double bond. This is followed by another smooth cation-mediated annulation to give the 5,5,6,5-tetracyclic skeleton **IM17**, which undergoes a 1,2-H shift via **TS_17−18a** to give **IM18a**. Then a C−C bond rearrangement takes place to yield the 5,6,5,5-tetraspirocyclic mangicol core skeleton (**IM14b**), which is subjected to a deprotonation to form **PD**. Notably, this new route is not only kinetically and thermodynamically the most favorable pathway but also appears to provide a versatile biosynthetic pathway leading to the formation of related terpenes/terpenoids, including tsukubadiene,[58] variediene,[54,55] deoxyconidiogenol/conidioge-

https://doi.org/10.1021/jacsau.1c00178
JACS Au 2021, 1, 1231−1239

none,[59,60] and phomopsene/methyl phomopsenonate[61,62] (Figure 5B,C). A careful structural comparison of the terpene cyclases responsible for the formation of mangicol, tsukubadiene, variediene, deoxyconidiogenol, and phomopsene could be helpful to clarify how the structural diversification is controlled.

CONCLUSION

In conclusion, the current computational study has uncovered in detail the biosynthetic pathways of the verrucosane-type diterpenoids and mangicol-type sesterterpenoids as well as provided new insight into the mechanisms of structure diversification in terpene biosynthesis, especially the exquisite skeletal construction processes and conformational changes (the Cartesian coordinates of the three-dimensional structures of all species are given in the Supporting Information). Remarkably, we found that none of the previously proposed 2° carbocation intermediates was obtained as a minimum on the PES. The verrucosane biosynthetic cascade bypasses the formation of unstable 2° carbocations **II** and **IV** by the formation of adjacent 3° carbocations (**IM1** and **IM3**) combined with skeletal rearrangement reactions involving reverse (3° → 2° cation) Wagner-Meerwein rearrangements. Other putative 2° cations were located in equilibrium with nonclassical carbocation intermediates (**IM5** and **IM7**) via viaa bicyclobutonium cation (**IM6**), and this could be the branching point between the verrucosan-2β-ol (**ver**) and neoverrucosan-5β-ol (**neo**) biosyntheses. In the mangicol cyclization cascade, the formation of putative 2° carbocation **X** is bypassed by breaking the adjacent C−C bond to form the more stable 3° carbocation (**IM10**). Although C−C bond cleavage is an endothermic reaction, the unfavorable energy loss is compensated by the simultaneous generation of a C═C double bond and a more stable 3° carbocation. Another proposed 2° carbocation **XI** is avoided as a result of a strong hyperconjugative interaction with the adjacent C−C bond, affording a nonclassical structure (**IM11**) between a 3° carbocation and a humulyl 2° cation. We further found a new, energetically viable pathway for the 6,5,5-spirotricycle formation in the mangicol biosynthesis, and this can also account for the formation of other terpenes/terpenenoids. A future comparative study of the terpene cyclases responsible for mangicol, tsukubadiene, variediene, deoxyconidiogenol, and phomopsene formations could help to establish the molecular basis of the regulation of the branching biosynthetic pathways by these enzymes. Thus, the results presented here are helpful to complete the picture of verrucosane and mangicol biosynthesis and also offer insights into the stability and reactivity of various carbocations and bonds that should be useful not only in terpene biosynthesis but also in fundamental organic chemistry. In particular, this work underlines that great caution is needed in suggesting the involvement of 2° carbocations (even in the cases of humulyl cations and cycloalkylcarbinyl cations) in the biosynthesis of natural products, since they are very unstable compared with 3° cations. We hope this work will be helpful for future mechanistic investigations of terpenes/terpenoids biosynthesis.

ASSOCIATED CONTENT

Supporting Information

The Supporting Information is available free of charge at https://pubs.acs.org/doi/10.1021/jacsau.1c00178.

Computational details, three-dimensional representation of the structure, coordinates and energies for all computed structures (PDF)

AUTHOR INFORMATION

Corresponding Authors

Masanobu Uchiyama − *Graduate School of Pharmaceutical Sciences, The University of Tokyo, Bunkyo-ku, Tokyo 113-0033, Japan; Research Initiative for Supra-Materials, Shinshu University, Nagano 386-8567, Japan;* orcid.org/0000-0001-6385-5944; Email: uchiyama@mol.f.u-tokyo.ac.jp

Hajime Sato − *Interdisciplinary Graduate School of Medicine and Engineering, University of Yamanashi, Kofu, Yamanashi 400-8510, Japan; Graduate School of Pharmaceutical Sciences, The University of Tokyo, Bunkyo-ku, Tokyo 113-0033, Japan;* orcid.org/0000-0001-5185-096X; Email: hsato@yamanashi.ac.jp

Authors

Bi-Xiao Li − *Graduate School of Pharmaceutical Sciences, The University of Tokyo, Bunkyo-ku, Tokyo 113-0033, Japan*

Taisei Takagi − *Graduate School of Pharmaceutical Sciences, The University of Tokyo, Bunkyo-ku, Tokyo 113-0033, Japan*

Chao Wang − *Graduate School of Pharmaceutical Sciences, The University of Tokyo, Bunkyo-ku, Tokyo 113-0033, Japan;* orcid.org/0000-0002-9165-7758

Kazunori Miyamoto − *Graduate School of Pharmaceutical Sciences, The University of Tokyo, Bunkyo-ku, Tokyo 113-0033, Japan;* orcid.org/0000-0003-1423-6287

Complete contact information is available at: https://pubs.acs.org/10.1021/jacsau.1c00178

Notes

The authors declare no competing financial interest.

ACKNOWLEDGMENTS

This work was supported by JSPS KAKENHI (S) (No. 17H06173 (M.U.)), MEXT Leading Initiative for Excellent Young Researchers (No. JPMXS0320200422 (H.S.)), JSPS Grant-in-Aid for Scientific Research on Innovative Areas (No. 19H04643 (M.U.)), and JST CREST (No. JPMJCR19R2 (M.U.)).

REFERENCES

(1) Christianson, D. W. Structural and Chemical Biology of Terpenoid Cyclases. *Chem. Rev.* **2017**, *117*, 11570−11648.

(2) Maeda, S.; Ohno, K.; Morokuma, K. Systematic Exploration of the Mechanism of Chemical Reactions: the Global Reaction Route Mapping (GRRM) Strategy Using the ADDF and AFIR methods. *Phys. Chem. Chem. Phys.* **2013**, *15*, 3683−3701.

(3) Isegawa, M.; Maeda, S.; Tantillo, D. J.; Morokuma, K. Predicting Pathways for Terpene Formation from First Principles-Routes to Known and New Sesquiterpenes. *Chem. Sci.* **2014**, *5*, 1555−1560.

(4) Sato, H.; Hashishin, T.; Kanazawa, J.; Miyamoto, K.; Uchiyama, M. DFT Study of a Missing Piece in Brasilane-Type Structure Biosynthesis: An Unusual Skeletal Rearrangement. *J. Am. Chem. Soc.* **2020**, *142*, 19830−19834.

(5) Sato, H.; Mitsuhashi, T.; Yamazaki, M.; Abe, I.; Uchiyama, M. Computational Studies on Biosynthetic Carbocation Rearrangements leading to Quiannulatene: Initial Conformation Regulates Biosynthetic Route, Stereochemistry, and Type of Skeleton. *Angew. Chem., Int. Ed.* **2018**, *57*, 14752−14757.

(6) Sato, H.; Teramoto, K.; Masumoto, Y.; Tezuka, N.; Sakai, K.; Ueda, S.; Totsuka, Y.; Shinada, T.; Nishiyama, M.; Wang, C.; Kuzuyama, T.; Uchiyama, M. "Cation-Stitching Cascade": Exquisite Control of Terpene Cyclization in Cyclooctatin Biosynthesis. *Sci. Rep.* **2016**, *5*, 18471−18476.
(7) Hong, Y. J.; Tantillo, D. J. The Energetic Viability of an Unexpected Skeletal Rearrangement in Cyclooctatin Biosynthesis. *Org. Biomol. Chem.* **2015**, *13*, 10273−10278.
(8) Olah, G. A.; Prakash, G. K. S. In *Carbocation Chemistry;* Wiley-VCH: Weinheim, Germany, 2004; pp 1−408.
(9) Carey, F. A.; Sundberg, R. J. In *Advanced Organic Chemistry;* Kluwer Academic: New York, 2000; pp 263−350.
(10) Deno, N. C.; Jaruzelski, J. J.; Schriesheim, A. Carbonium Ions. I. An Acidity Function (C0) Derived from Arylcarbonium Ion Equilibria. *J. Am. Chem. Soc.* **1955**, *77*, 3044−3051.
(11) Bittner, E. W.; Arnett, E. M.; Saunders, M. Quantitative Preparation and Enthalpy of Rearrangement of the *sec*-Butyl Cation. *J. Am. Chem. Soc.* **1976**, *98*, 3734−3735.
(12) Hefter, J.; Richnow, H. H.; Fischer, U.; Trendel, J. M.; Michaelis, W. (−)-Verrucosan-2β-ol from the Phototrophic Bacterium *Chloroflexus aurantiacus*: First Report of a Verrucosane-type Diterpenoid from a Prokaryote. *J. Gen. Microbiol.* **1993**, *139*, 2757−2761.
(13) Rieder, C.; Strauss, G.; Fuchs, G.; Arigoni, D.; Bacher, A.; Eisenreich, W. Biosynthesis of the Diterpene Verrucosan-2β-ol in the Phototrophic Eubacterium Chloroflexus aurantiacus. *J. Biol. Chem.* **1998**, *273*, 18099−18108.
(14) Eisenreich, W. C.; Rieder, C.; Grammes, C.; Hessler, G.; Adam, K. P.; Becker, H.; Arigoni, D.; Bacher, A. Biosynthesis of a Neo-*epi*-verrucosane Diterpene in the Liverwort *Fossombronia alaskana*. *J. Biol. Chem.* **1999**, *274*, 36312−36320.
(15) Yang, Y. L.; Zhang, S.; Ma, K.; Xu, Y.; Tao, Q.; Chen, Y.; Chen, J.; Guo, S.; Ren, J.; Wang, W.; Tao, Y.; Yin, W. B.; Liu, H. Discovery and Characterization of a New Family of Diterpene Cyclases in Bacteria and Fungi. *Angew. Chem., Int. Ed.* **2017**, *56*, 4749−4752.
(16) Renner, M. K.; Jensen, P. R.; Fenical, W. Mangicols: Structures and Biosynthesis of a New Class of Sesterterpene Polyols from a Marine Fungus of the Genus Fusarium. *J. Org. Chem.* **2000**, *65*, 4843−4852.
(17) Bian, G.; Han, Y.; Hou, A.; Yuan, Y.; Liu, X.; Deng, Z.; Liu, T. Releasing the Potential Power of Terpene Synthases by a Robust Precursor Supply Platform. *Metab. Eng.* **2017**, *42*, 1−8.
(18) Maeda, S.; Osada, Y.; Morokuma, K.; Ohno, K. *GRRM11,* ver. 11.03; Institute for Quantum Chemical Exploration, 2012.
(19) Ohno, K.; Maeda, S. A Scaled Hypersphere Search Method for the Topography of Reaction Pathways on the Potential Energy Surface. *Chem. Phys. Lett.* **2004**, *384*, 277−282.
(20) Maeda, S.; Ohno, K. Global Mapping of Equilibrium and Transition Structures on Potential Energy Surfaces by the Scaled Hypersphere Search Method: Applications to *ab initio* Surfaces of Formaldehyde and Propyne Molecules. *J. Phys. Chem. A* **2005**, *109*, 5742−5753.
(21) Ohno, K.; Maeda, S. Global Reaction Route Mapping on Potential Energy Surfaces of Formaldehyde, Formic Acid, and Their Metal-Substituted Analogues. *J. Phys. Chem. A* **2006**, *110*, 8933−8941.
(22) Frisch, M. J.; et al. *Gaussian 16,* rev. C.01; Gaussian, Inc.: Wallingford, CT, 2016 (full reference is in the Supporting Information).
(23) Zhao, Y.; Truhlar, D. G. The M06 Suite of Density Functionals for Main Group Thermochemistry, Thermochemical Kinetics, Noncovalent Interactions, Excited States, and Transition Elements: Two New Functionals and Systematic Testing of Four M06-class Functionals and 12 Other Functionals. *Theor. Chem. Acc.* **2008**, *120*, 215−241.
(24) Fukui, K. The Path of Chemical Reactions - The IRC Approach. *Acc. Chem. Res.* **1981**, *14*, 363−368.
(25) Page, M.; Doubleday, C.; McIver, J. W., Jr. Following Steepest Descent Reaction Paths. The Use of Higher Energy Derivatives with *ab initio* Electronic Structure Methods. *J. Chem. Phys.* **1990**, *93*, 5634−5642.
(26) Ishida, K.; Morokuma, K.; Komornicki, A. The Intrinsic Reaction Coordinate. An *ab initio* Calculation for HNC→HCN and $H^- + CH_4 \rightarrow CH_4 + H^-$. *J. Chem. Phys.* **1977**, *66*, 2153−2156.
(27) Gonzalez, C.; Schlegel, H. B. Reaction Path Following in Mass-weighted Internal Coordinates. *J. Phys. Chem.* **1990**, *94*, 5523−5527.
(28) Adamo, C.; Barone, V. Exchange Functionals with Improved Long-range Behavior and Adiabatic Connection Methods without Adjustable Parameters: The mPW and mPW1PW Models. *J. Chem. Phys.* **1998**, *108*, 664−675.
(29) Matsuda, S. P. T.; Wilson, W. K.; Xiong, Q. Mechanistic Insights into Triterpene Synthesis from Quantum Mechanical Calculations. Detection of Systematic Errors in B3LYP Cyclization Energies. *Org. Biomol. Chem.* **2006**, *4*, 530−543.
(30) Croteau, R. B.; Shaskus, J. J.; Renstrom, B.; Felton, N. M.; Cane, D. E.; Saito, A.; Chang, C. Mechanism of the Pyrophosphate Migration in the Enzymatic Cyclization of Geranyl and Linalyl Pyrophosphates to (+)- and (−)-Bornyl Pyrophosphates. *Biochemistry* **1985**, *24*, 7077−7085.
(31) Hong, Y. J.; Tantillo, D. J. Quantum Chemical Dissection of the Classic Terpinyl/Pinyl/Bornyl/Camphyl Cation Conundrum - The Role of Pyrophosphate in Manipulating Pathways to Monoterpenes. *Org. Biomol. Chem.* **2010**, *8*, 4589−4600.
(32) Mazur, R. H.; White, W. N.; Semenow, D. A.; Lee, C. C.; Silver, M. S.; Roberts, J. D. Small-ring Compounds. XXIII. The Nature of the Intermediates in Carbonium Ion-type Interconversion Reactions of Cyclopropylcarbinyl, Cyclobutyl and Allylcarbinyl Derivatives. *J. Am. Chem. Soc.* **1959**, *81*, 4390−4398.
(33) Hong, Y. J.; Giner, J.-L.; Tantillo, D. J. Bicyclobutonium Ions in Biosynthesis − Interconversion of Cyclopropyl-Containing Sterols from Orchids. *J. Am. Chem. Soc.* **2015**, *137*, 2085−2088.
(34) Nozoe, S.; Morisaki, M.; Tsuda, K.; Iitaka, Y.; Takahashi, N.; Tamura, S.; Ishibashi, K.; Shirasaka, M. The Structure of Ophiobolin, a C25 Terpenoid Having a Novel Skeleton. *J. Am. Chem. Soc.* **1965**, *87*, 4968−4970.
(35) Chiba, R.; Minami, A.; Gomi, K.; Oikawa, H. Identification of Ophiobolin F Synthase by a Genome Mining Approach: A Sesterterpene Synthase from *Aspergillus clavatus*. *Org. Lett.* **2013**, *15*, 594−597.
(36) Sassa, T.; Ooi, T.; Nukita, M.; Ikeda, M.; Kato, N. Structural Confirmation of Cotylenin A, a Novel Fusicoccane-diterpene Glycoside with Potent Plant Growth-regulating Activity from *Cladosporium* Fungus sp. 501−7W. *Biosci. Biotechnol. Biochem.* **1998**, *62*, 1815−1818.
(37) Toyomasu, T.; Tsukahara, M.; Kaneko, A.; Niida, R.; Mitsuhashi, W.; Dairi, T.; Kato, N.; Sassa, T. Fusicoccins are Biosynthesized by an Unusual Chimera Diterpene Synthase in Fungi. *Proc. Natl. Acad. Sci. U. S. A.* **2007**, *104*, 3084−3088.
(38) Minami, A.; Ozaki, T.; Liu, C.; Oikawa, H. Cyclopentane-forming Di/Sesterterpene Synthases: Widely Distributed Enzymes in Bacteria, Fungi, and Plants. *Nat. Prod. Rep.* **2018**, *35*, 1330−1346.
(39) Okada, M.; Matsuda, Y.; Mitsuhashi, T.; Hoshino, S.; Mori, T.; Nakagawa, K.; Quan, Z.; Qin, B.; Zhang, H.; Hayashi, F.; Kawaide, H.; Abe, I. Genome-Based Discovery of an Unprecedented Cyclization Mode in Fungal Sesterterpenoid Biosynthesis. *J. Am. Chem. Soc.* **2016**, *138*, 10011−10018.
(40) Ye, Y.; Minami, A.; Mandi, A.; Liu, C.; Taniguchi, T.; Kuzuyama, T.; Monde, K.; Gomi, K.; Oikawa, H. Genome Mining for Sesterterpenes Using Bifunctional Terpene Synthases Reveals a Unified Intermediate of Di/Sesterterpenes. *J. Am. Chem. Soc.* **2015**, *137*, 11846−11853.
(41) Sato, H.; Narita, K.; Minami, A.; Yamazaki, M.; Wang, C.; Suemune, H.; Nagano, S.; Tomita, T.; Oikawa, H.; Uchiyama, M. Theoretical Study of Sesterfisherol Biosynthesis: Computational Prediction of Key Amino Acid Residue in Terpene Synthase. *Sci. Rep.* **2018**, *8*, 2473−2481.
(42) Huang, A. C.; Kautsar, S. A.; Hong, Y. J.; Medema, M. H.; Bond, A. D.; Tantillo, D. J.; Osbourn, A. Unearthing a Sesterterpene

Biosynthetic Repertoire in the Brassicaceae through Genome Mining Reveals Convergent Evolution. *Proc. Natl. Acad. Sci. U. S. A.* **2017**, *114*, E6005−E6014.
(43) Huang, A. C.; Hong, Y. J.; Bond, A. D.; Tantillo, D. J.; Osbourn, A. Diverged Plant Terpene Synthases Reroute the Carbocation Cyclization Path towards the Formation of Unprecedented 6/11/5 and 6/6/7/5 Sesterterpene Scaffolds. *Angew. Chem., Int. Ed.* **2018**, *57*, 1291−1295.
(44) Hou, A.; Dickschat, J. S. The Biosynthetic Gene Cluster for Sestermobaraenes—Discovery of a Geranylfarnesyl Diphosphate Synthase and a Multiproduct Sesterterpene Synthase from Streptomyces Mobaraensis. *Angew. Chem., Int. Ed.* **2020**, *59*, 19961−19965.
(45) Guo, J.; Cai, Y. S.; Cheng, F.; Yang, C.; Zhang, W.; Yu, W.; Yan, J.; Deng, Z.; Hong, K. Genome Mining Reveals a Multiproduct Sesterterpenoid Biosynthetic Gene Cluster in *Aspergillus Ustus*. *Org. Lett.* **2021**, *23*, 1525−1529.
(46) Hess, B. A. Concomitant C-Ring Expansion and D-Ring Formation in Lanosterol Biosynthesis from Squalene without Violation of Markovnikov's Rule. *J. Am. Chem. Soc.* **2002**, *124*, 10286−10287.
(47) Hess, B. A. Formation of the C Ring in the Lanosterol Biosynthesis from Squalene. *Org. Lett.* **2003**, *5*, 165−167.
(48) Hess, B. A.; Smentek, L. Concerted Nature of AB Ring Formation in the Enzymatic Cyclization of Squalene to Hopenes. *Org. Lett.* **2004**, *6*, 1717−1720.
(49) Hess, B. A., Jr.; Smentek, L. The Concerted Nature of the Cyclization of Squalene Oxide to the Protosterol Cation. *Angew. Chem., Int. Ed.* **2013**, *52*, 11029−11033.
(50) A similar hyperconjugative interaction has been observed in abietadiene biosynthesis, see: Tantillo, D. J. The Carbocation Continuum in Terpene Biosynthesis—Where are the Secondary Cations? *Chem. Soc. Rev.* **2010**, *39*, 2847−2854.
(51) Hong, Y. J.; Tantillo, D. J. A Potential Energy Surface Bifurcation in Terpene Biosynthesis. *Nat. Chem.* **2009**, *1*, 384−389.
(52) Rabe, P.; Samborskyy, M.; Leadlay, P. F.; Dickschat, J. S. Isoafricanol Synthase from Streptomyces Malaysiensis. *Org. Biomol. Chem.* **2017**, *15*, 2353−2358.
(53) Scholz, F.; Himmel, D.; Heinemann, F. W.; Schleyer, R.; Meyer, K.; Krossing, I. Crystal Structure Determination of the Nonclassical 2-Norbornyl Cation. *Science* **2013**, *341*, 62−64.
(54) Rinkel, J.; Steiner, S. T.; Bian, G.; Chen, R.; Liu, T.; Dickschat, J. S. A Family of Related Fungal and Bacterial Di- and Sesterterpenes: Studies on Fusaterpenol and Variediene. *ChemBioChem* **2020**, *21*, 486−491.
(55) Hong, Y. J.; Tantillo, D. J. The Variediene-Forming Carbocation Cyclization/Rearrangement Cascade. *Aust. J. Chem.* **2017**, *70*, 362−366.
(56) Winstein, S.; Holness, N. J. Neighboring Carbon and Hydrogen. XVIII. Solvolysis of the Nopinyl *p*-Bromobenzenesulfonates. *J. Am. Chem. Soc.* **1955**, *77*, 3054−3061.
(57) Yamato, T.; Fujita, K.; Shinoda, N.; Noda, K.; Nagano, Y.; Arimura, T.; Tashiro, M. Through-space Electronic Interactions of [2.2]Metacyclophane Benzyl Cations. *Res. Chem. Intermed.* **1996**, *22*, 871−897.
(58) Rabe, P.; Rinkel, J.; Dolja, E.; Schmitz, T.; Nubbemeyer, B.; Luu, T. H.; Dickschat, J. S. Mechanistic Investigations of Two Bacterial Diterpene Cyclases: Spiroviolene Synthase and Tsukubadiene Synthase. *Angew. Chem., Int. Ed.* **2017**, *56*, 2776−2779.
(59) Roncal, T.; Cordobés, S.; Sterner, O.; Ugalde, U. Conidiation in Penicillium Cyclopium is Induced by Conidiogenone, an Endogenous Diterpene. *Eukaryotic Cell* **2002**, *1*, 823−829.
(60) Mitsuhashi, T.; Kikuchi, T.; Hoshino, S.; Ozeki, M.; Awakawa, T.; Shi, S. P.; Fujita, M.; Abe, I. Crystalline Sponge Method Enabled the Investigation of a Prenyltransferase-Terpene Synthase Chimeric Enzyme, Whose Product Exhibits Broadened NMR Signals. *Org. Lett.* **2018**, *20*, 5606−5609.
(61) Toyomasu, T.; Kaneko, A.; Tokiwano, T.; Kanno, Y.; Kanno, Y.; Niida, R.; Miura, S.; Nishioka, T.; Ikeda, C.; Mitsuhashi, W.; Dairi, T.; Kawano, T.; Oikawa, H.; Kato, N.; Sassa, T. Biosynthetic Gene-Based Secondary Metabolite Screening: a New Diterpene, Methyl Phomopsenonate, from the Fungus *Phomopsis amygdali*. *J. Org. Chem.* **2009**, *74*, 1541−1548.
(62) Lauterbach, L.; Rinkel, J.; Dickschat, J. S. Two Bacterial Diterpene Synthases from *Allokutzneria albata* Produce Bonnadiene, Phomopsene, and Allokutznerene. *Angew. Chem., Int. Ed.* **2018**, *57*, 8280−8283.

https://doi.org/10.1021/jacsau.1c00178
JACS Au 2021, 1, 1231−1239